

Printing of Conductive and Insulating Structures with Micrometer Resolution for Next-Generation Displays

Aneta Wiatrowska, Piotr Kowalczewski, Karolina Fińczyk, Łukasz Witczak, Jolanta Gadzalińska, Iwona Grądzka-Kurzaj, Mateusz Łysień, Ludovic Schneider, Łukasz Kosior, Filip Granek

piotr.kowalczewski@xtpl.com

XTPL SA, Stabłowicka 147, 54-066 Wrocław, Poland

Keywords: ultraprecise deposition, micrometer-size conductive structures, high-viscosity nanoparticle inks

ABSTRACT

We demonstrate the versatility of the Ultra-Precise Deposition approach for rapid-prototyping of next-generation displays. We focus on how to print conductive and non-conductive materials at micrometer scale to fabricate different building-blocks of high-resolution displays.

1 Introduction

In our previous contributions [1], [2] we presented the Ultra-Precise Deposition (UPD) technology [3] to print micrometric conductive structures for high-resolution flat panel displays. In this contribution we demonstrate progress in the development of this method and highlight versatility of the UPD approach for rapid-prototyping of next-generation displays. We will show how UPD can be used to fabricate various display components, such as fine metal masks for OLED displays [4]; highly-conductive electrical interconnectors for high-resolution displays [5]; gate/source/drain in thin-film transistor (TFT) arrays [6]; precisely-deposited adhesion layers for metal electrodes [7]; or photoresist molds in quantum dot (QD) and OLED displays [8].

Prototyping different display components using the UPD approach is possible because this method is compatible with a wide range of conductive and non-conductive materials, including silver, gold, and copper pastes, as well as insulating materials, like photoresists. In addition, one can print high-viscosity pastes on substrates with pre-existing features, like steps much higher than width of the printed line.

2 Ultra-precise deposition

UPD process is based on the direct extrusion of conductive or insulating materials using pressure, as sketched in Figure 1. Different classes of materials can be printed: from low viscosity metallic and non-conductive inks to high-viscosity non-Newtonian pastes. The process is controlled by a number of parameters, including the value of pressure, printing speed, and the position of the nozzle opening with respect to the substrate. In Fig. 2 we show line width as a function of the printing pressure and printing speed for the nozzle with the opening of 3.5 μm , printed using paste based on silver nanoparticles. It can

be seen that the smallest structures (width equal to 1 μm) are achieved for the combination of low pressure and high printing speed. Missing data points in the top left corner (gray region) for lines with the width below 1 μm show the current limit of this technology. The distance between the nozzle opening and the substrate is controlled using a vision algorithm.

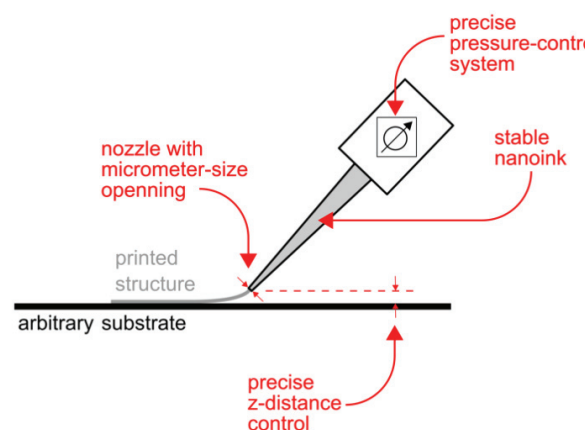


Figure 1. Sketch demonstrating the UPD technique. The ink is extruded from a micrometer-size nozzle using pressure, and the material is directly deposited on the substrate

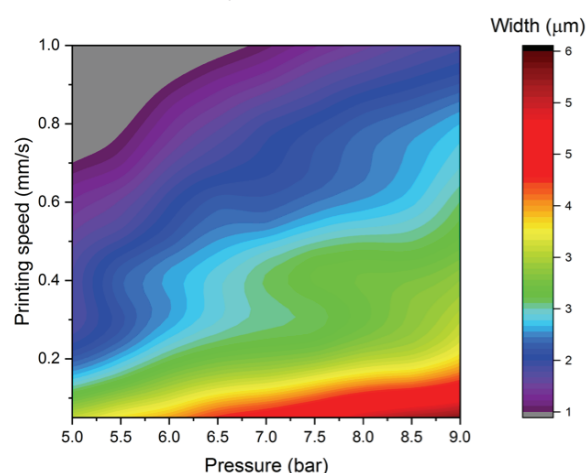


Figure 2. Line width as a function of the printing pressure and printing speed for the printing nozzle with the opening of 3.5 μm

3 Results

3.1 High-Resolution Printing

In Fig. 3a) we show silver lines with the width of $3\ \mu\text{m}$ and interline spacing of $0.7\ \mu\text{m}$. The lines are printed on a flexible substrate, i.e., PET foil. Although the lines are separated by less than $1\ \mu\text{m}$, it can be seen that there are no short-circuits. Interline distance below $1\ \mu\text{m}$ may allow to obtain, for example, narrow channels in printed transistors. Magnified view of the sample is shown in the inset.

In Fig. 3b) we demonstrate high density of printed lines: the pattern is made of $5\ \mu\text{m}$ wide silver lines with the interline distance equal to $5\ \mu\text{m}$. The shape also demonstrates the capability of printing in different directions, without artifacts at the corners.

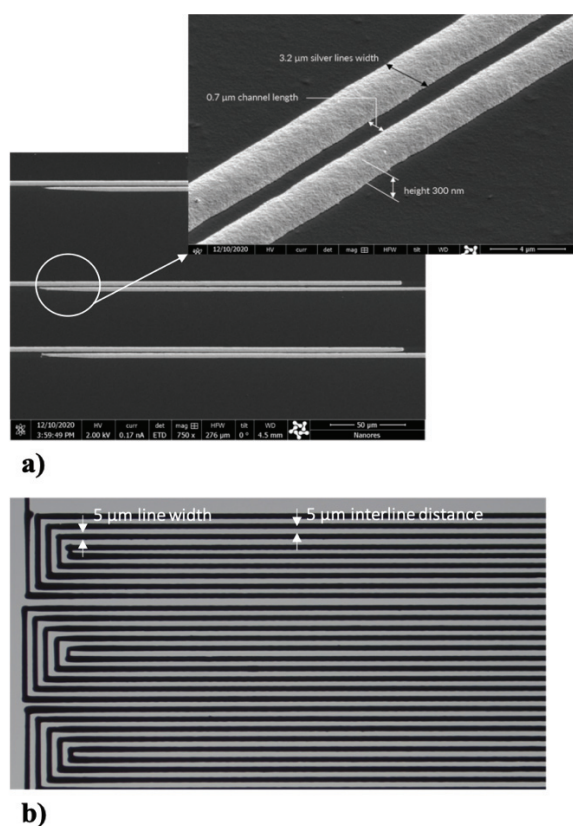


Figure 3. a) Silver lines with the width of $3\ \mu\text{m}$ printed on a PET foil. The interline spacing is $0.7\ \mu\text{m}$. Magnified view of the sample is shown in the inset; **b)** demonstration of high line density: the pattern made of $5\ \mu\text{m}$ wide silver lines with the interline distance equal to $5\ \mu\text{m}$.

3.2 Conductive meshes

Conductive meshes are a vital part of rigid and flexible displays, as well as e-paper, transparent displays, and smart devices. However, the choice of the conductive material depends on various design constraints, cost analysis, specific architecture, and compatibility with other components of the device. In Fig. 4 we show example

conductive meshes printed using different materials. In Fig. 4a) we demonstrate a conductive mesh with $5\ \mu\text{m}$ wide lines printed using paste based on silver nanoparticles (85 wt. % of solid content). The whole sample is shown in the inset.

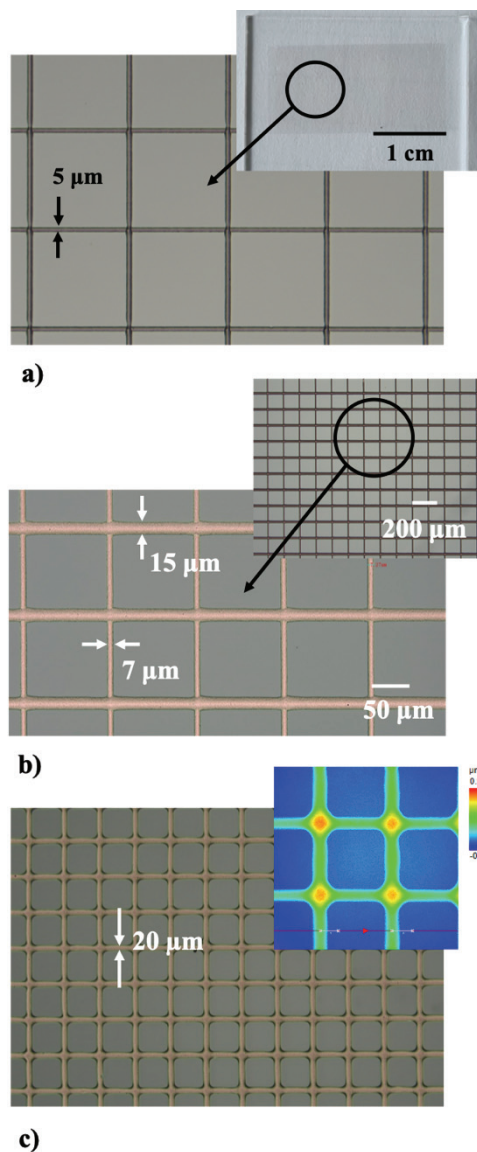


Figure 4. a) Conductive mesh with $5\ \mu\text{m}$ wide lines, printed using silver paste. The whole sample is shown in the inset; **b)** conductive mesh printed using copper paste. The inset shows distant view of the sample; **c)** conductive mesh printed using gold paste. In the inset we show a heat map corresponding to the height profile

In Fig. 4b) we show a conductive mesh printed using copper paste (80 wt. % of solid content). In this design the lines have various widths: $7\ \mu\text{m}$ in the horizontal direction and $15\ \mu\text{m}$ in the vertical direction. The inset shows lower magnification of the sample.

Finally, in Fig. 4c) we present a conductive mesh

printed using gold paste (80 wt. % of solid content). In the inset we show a heat map corresponding to the height profile.

3.3 Insulating Materials

Up to now we have discussed printing using high-viscosity conductive materials developed in-house. In this section we focus on insulating materials obtained from external suppliers. In Fig. 5 we show an array of microdots printed with photoresist AR-P 3110 (obtained from: Allresist GmbH). This material is characterized by the viscosity of 12 cP, therefore orders of magnitude lower than in the case of the conductive pastes. The distance between the printed dots is equal to 50 μm , the dot diameter is equal to 13 μm , and the dot height is equal to 10 μm . The microdots are characterized by parabolic shape, which may, for example, simplifying the deposition of subsequent layers without the risk of cracks.

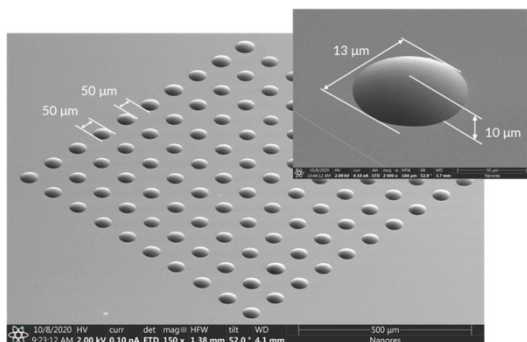


Figure 5. Array of microdots printed with photoresist AR-P 3110, characterized by the viscosity of 12 cP

3.4 Printing on Steps

In Fig. 6 we demonstrate the capabilities of the UPD technology to print on steps with various heights: repeatable and continuous silver lines with a width of 15 μm are printed on the step with the height of 150 μm . Therefore, the step height is ten times the width of the lines. This gives the possibility to fabricate 3D interconnections for advanced packaging, including hybrid electronics (combining printed electronics and silicon technologies).

4 Conclusions

In this contribution we discuss the UPD technology for rapid prototyping of high-resolution displays. To highlight the versatility of this method, we give a number of examples of printing using different conductive and non-conductive materials to obtain various display components. Based on these results, we argue that UPD can be used to increase the productivity and decrease the costs of the development of next-generation displays.

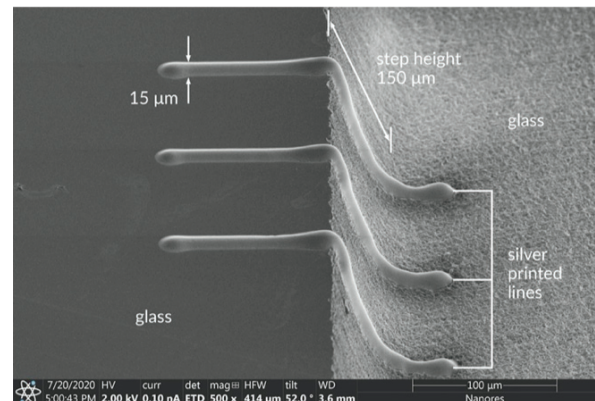


Figure 6. Repeatable and continuous silver lines with a width of 15 μm printed on the step with the height of 150 μm

References

- [1] A. Wiatrowska, "Ultra-Precise Deposition Technology for High-Resolution Flat Panel Displays," presented at the International Display Workshops General Incorporated Association, Sep. 2020. doi: 10.36463/idw.2020.0232.
- [2] A. Wiatrowska *et al.*, "High Resolution Printing of Conducting Lines in μm Range," presented at the International Display Workshops General Incorporated Association, Sep. 2021. doi: 10.36463/idw.2021.0249.
- [3] M. Łysień *et al.*, "High-resolution deposition of conductive and insulating materials at micrometer scale on complex substrates," *Sci. Rep.*, vol. 12, no. 1, pp. 1–18, 2022.
- [4] M. Mizukami *et al.*, "Flexible Organic Light-Emitting Diode Displays Driven by Inkjet-Printed High-Mobility Organic Thin-Film Transistors," *IEEE Electron Device Lett.*, vol. 39, no. 1, pp. 39–42, Jan. 2018, doi: 10.1109/LED.2017.2776296.
- [5] T. Zhan, K. Yin, J. Xiong, Z. He, and S.-T. Wu, "Augmented Reality and Virtual Reality Displays: Perspectives and Challenges," *iScience*, vol. 23, no. 8, p. 101397, Aug. 2020, doi: 10.1016/j.isci.2020.101397.
- [6] E. Sowade *et al.*, "Up-scaling of the manufacturing of all-inkjet-printed organic thin-film transistors: Device performance and manufacturing yield of transistor arrays," *Org. Electron.*, vol. 30, pp. 237–246, Mar. 2016, doi: 10.1016/j.orgel.2015.12.018.
- [7] B. F. E. Matarèse, P. L. C. Feyen, A. Falco, F. Benfenati, P. Lugli, and J. C. deMello, "Use of SU8 as a stable and biocompatible adhesion layer for gold bioelectrodes," *Sci. Rep.*, vol. 8, no. 1, p. 5560, Apr. 2018, doi: 10.1038/s41598-018-21755-6.
- [8] H.-J. Kim *et al.*, "Enhancement of Optical Efficiency in White OLED Display Using the Patterned Photoresist Film Dispersed With Quantum Dot Nanocrystals," *J. Disp. Technol.*, vol. 12, no. 6, pp. 526–531, Jun. 2016, doi: 10.1109/JDT.2015.2503401.